Pillared Clays as a New Class of Sorbents for Gas Separation

R. T. Yang and M. S. A. Baksh
Dept. of Chemical Engineering, State University of New York, Buffalo, NY 14260

High-surface-area, Zr-pillared, layered clays are synthesized and characterized for their adsorption properties. Although large free interlayer spacings are claimed in the literature (as also found in this work, 14.3 Å), the limiting pore size is the narrow interpillar spacing. The distribution of interpillar spacing is determined by molecular probing and adsorption data along with a theoretical framework available from the literature. Interpillar spacing can be tailored by controlling the number density of pillars inserted during the ion exchange (oligomer inserting) step. The following variables in the ion exchange solution result in lowering the pillar density: higher pH, lower oligomer concentration, and introduction of competitive cations. By changing these variables, peak interpillar spacing is shifted by nearly 2 Å (from 5 to 7 Å). The versatility of pillared clays as sorbents for kinetic separation (i.e., separation based on diffusivity differences) has been demonstrated by the separations of air and xylene isomers.

Introduction

Pillared interlayered clays (PILC), or pillared clays, are two-dimensional zeolite-like materials prepared by exchanging charge-compensating cations between the clay layers with large inorganic hydroxycations, which are polymeric or oligomeric hydroxy metal cations formed by hydrolysis of metal oxides or salts. Upon heating, metal hydroxycations undergo dehydration and dehydroxylation, forming stable metal oxide clusters that act as pillars, keeping the silicate layers separated and creating interlayer space (gallery) of molecular dimensions. Much interest and research have been directed to PILC since their first successful syntheses in the late 1970s (Brindley and Semples, 1977; Vaughan et al., 1979; Lahav et al., 1978; Loeppert et al., 1979; Shabtai et al., 1980; Occelli and Tindwa, 1983). Comprehensive reviews of the voluminous literature on the subject are available (Pinnavaia, 1983; Burch, 1988; Figueras, 1988). In principle, any metal oxide or salt that forms polynuclear species upon hydrolysis (Baes and Mesmer, 1976) can be inserted as pillars, and all layered clays of the abundant phyllosilicate family as well as other layered clays can be used as the hosts (see references cited in Burch, 1988; Clearfield, 1988; Drezdzon, 1988; Sprung et al., 1990). The two most extensively studied and best understood pillared clays are montmorillonite pillared by alumina and zirconia.

The literature on PILC deals almost exclusively with catalytic applications (Pinnavaia, 1983; Burch, 1988; Figueras, 1988). The short list of "sorbent" studies is limited to a small number of adsorption isotherm measurements (Occelli et al., 1985; Bandoz et al., 1989; Tzou and Pinnavaia, 1988; Yamanaka and Hattori, 1988) and diffusivity studies (Occelli et al., 1985; Tsou and Pinnavaia, 1988; Sahimi et al., 1988). Physical characterization of PILC has been limited to interlayer spacing (from XRD data), surface area and, in a few instances, molecular probe studies (Shabtai et al., 1984; Tzou and Pinnavaia, 1988). From the low diffusivities in the pillared clays and the molecular probe results reported in the literature, it is clear that the pore sizes in the pillared clays are not limited by large interlayer spacings (up to about 20 Å), but are limited by interpillar spacings. The pore structure and the pore-size distribution in pillared clays, however, have not been studied and remain unknown.

Recent developments in adsorption have prompted a large number of applications for gas separation (Yang, 1987). Kinetic separation is a new class of separation processes in which separation is caused by differences in diffusion rates into the sorbent. A commercial application of kinetic separation is the generation of nitrogen from air by using molecular sieve carbon, in which O_2 diffuses faster than N_2, thus separating N_2 from air (Yang, 1987). Other promising kinetic separations

include CO_2/CH_4 separation (Kapoor and Yang, 1989), and N_2/CH_4 separation (Ackley and Yang, 1990), both by molecular sieve carbon and air separation by 4A zeolite (Shin and Knaebel, 1988; Pan et al., 1989). The success of kinetic separation depends critically on the sorbent. Conventional sorbents are not suitable for this purpose. Zeolites do not have a distribution of pore sizes and separate gases mainly by virtue of molecular exclusion. Molecular sieve carbon, with a distribution of pore sizes centered around approximately 5 Å, is the only viable sorbent for kinetic separation. In this article, we demonstrate that pillared clays also possess a distribution of micropores and report first kinetic separation results by a pillared clay. Furthermore, the results will be shown that the pore-size distribution in pillared clays can be tailored readily for specific separations.

Experimental Studies

Zr-PILC synthesis

The starting material for preparation of zirconium pillared clay (Zr-PILC) was a purified montmorillonite, purified-grade bentonite powder from Fisher Company, which is less than or equal to 2 μm in size. Zirconyl chloride ($ZrOCl_2 \cdot 8H_2O$), also from Fisher, was the salt to be hydrolyzed and used as the pillaring agent. Compounds used as probe molecules were of ACS certified grades from Fisher. All gases were from Union Carbide Linde Division, with a minimum purity of 99.9%.

The first step in PILC synthesis is the preparation and aging of the pillaring solution. The pillaring agent undergoes hydrolysis, polymerization and complexation with anions in the solution (Baes and Mesmer, 1976; Jones, 1988; Sterte, 1988; Bartley, 1988). The hydrolysis conditions are important to the formation of PILC: temperature, pH, and aging time. The oligomeric solution was prepared from zirconyl chloride octahydrate ($ZrOCl_2 \cdot 8H_2O$) by dissolving the equivalent amount of the salt in de-ionized, distilled water to produce a 0.1 M solution. This solution was aged at room temperature for 10 days at a pH of 1.3. The results in Table 1 give a value of 102.7 mEq/100 g of the cation exchange capacity of the bentonite clay (assuming that the only exchangeable cations are Na^+, Ca^{2+}, and K^+). In the synthesis of Zr-PILC, the pillaring stoichiometry should be at least 2.5 mmol Zr/1 g clay. Typically, 25 cm^3 of 0.1 M $ZrOCl_2$ should be used per 1.0 g of the Bentonite clay. The main intercalating species was the tetramer, $Zr_4(OH)_{14}(H_2O)_{10}^{2+}$. However, larger oligomers containing 20 to 40 metal ions were undoubtedly formed (Baes and Mesmer, 1976). The next step is intercalation (or ion exchange) of the small cations (e.g., Na^+) between the clay layers with oligomers. This was done by preparing the slurry that consisted of a suspension of the clay in de-ionized and distilled water, oligomeric solution, and HCl and/or NaOH used for pH adjustment. The pH of the clay/water suspension was 9.10 (1 g clay + 100 mL H_2O). The equivalent volume of the oligomeric solution, normally 25 cm^3, was added dropwise to the 1 g clay suspension, while vigorous stirring was maintained. Slow addition of the solution helped form uniform pillared clays. The pH of the resulting solution was checked and adjusted to the desired value using 0.1 M HCl or 0.1 M NaOH. The adjusted pH of the slurries used in this study was in the range 1.4–8.35. Ion exchange in the slurry took place at 50°C in a constant temperature bath shaker for a period of 3 days. Upon completion of ion exchange/intercalation, the sample was separated and washed by vacuum filtration. The residue on the filter was washed repeatedly with de-ionized and distilled water until no chloride ions remained as indicated by no further precipitation with $AgNO_3$ added to the filtrate. The final step was drying/calcination. The method and condition of the drying step have a strong influence on the porosity of the PILC (Pinnavaia et al., 1984). A three-step calcination (in air) was followed in this work: 100°C for 4 h, 200°C for 10 h, and 350°C for 24 h. The final PILC product was in an agglomerated form, which was ground and sieved for further use. The solution aging and ion exchange conditions described above were the conditions that resulted in Zr-PILC of the highest BET surface areas. Other conditions were also used (pH, temperature, time), but the results are not given here.

Table 1. Chemical Compositions of Clay and Zr-Pillared Clays

	wt. %			
	Bentonite	Zr-PILC-2	Zr-PILC-4	Zr-PILC-6
SiO_2	54.72	48.75	51.49	45.62
Al_2O_3	15.98	14.01	14.98	12.95
MgO	1.94	1.50	1.70	1.61
Fe_2O_3	2.93	2.49	2.78	2.44
TiO_2	0.12	0.12	0.19	0.12
Na_2O	2.04	0.22	0.39	1.39
CaO	0.82	0.09	0.40	0.72
ZrO_2	0.03	17.65	15.60	13.83
K_2O	0.34	0.27	0.23	0.26

Zr-PILC characterization

Chemical compositions of the clay samples were determined by a Thermo Jarrel Ash 61 inductively coupled argon plasma (ICP) atomic emission spectrometer. The sample was delivered to the nebulizer at a specified flow rate and was carried to the plasma by the carrier gas (argon). All elemental concentrations, except for zirconium, were determined by the polychromator, while zirconium was measured by the monochromator attachment using a wavelength setting of 389.2 nm. The instrument was calibrated using standard solutions. Clay samples were prepared for the ICP analysis using a fusion dissolution technique. Each sample of 100 mg was combined thoroughly with 0.6 g of a 1:2 lithium metaborate-lithium tetraborate fluxing mixture. This dry powder mixture was then placed in a graphite crucible and fused at 1,000°C. After cooling, the fused glass bead was added to a hot 250-cm^3 solution containing 10 cm^3 of a 1:1 HNO_3. The solution was filtered to remove graphite fibers prior to the ICP analysis.

The X-ray diffraction patterns were measured with a Nicolet/Stoe powder diffractomer with a position-sensitive detector. To maximize the 001 reflection intensities, oriented specimens were prepared for XRD by spreading wetted crystals on glass slides.

A Quantasorb surface area analyzer (Quantachrome Corp.) was used for BET surface area measurements. Prior to each measurement, the sample was outgassed at 200°C for 15 h. The N_2 isotherms (at 77 K) were also used for pore-size distribution calculations.

Isotherm and diffusivity measurements

Equilibrium adsorption isotherms and uptake rate curves were measured by using a microbalance (Mettler TA 2000 C thermoanalyzer), which was connected to a gas flow system. The flow system and the experimental procedures were the same as that described elsewhere (Yeh and Yang, 1989). Stringent steps were taken in the design, calibration and operation of the TGA/flow system to minimize or eliminate the undesirable factors, which often plague the measurement of diffusivities in zeolite: nonisothermal effect, external resistance, and traces of moisture. The carrier gas (helium) and adsorptive gases were purified and dried by passing through presorbers before entering the balance. A gas chromatograph with FID or TC detector (depending on the adsorptive gas) was used to measure the gas composition. Gas wash bottles (bubblers) were used to generate vapors from liquid adsorptives. Samples of less than 50 mg were used. Further details are given in Yeh and Yang (1989).

Since the PILC are two-dimensional materials, the uptake curves were fitted to the standard solution of a two-dimensional diffusion equation to obtain diffusivities. These diffusivities are approximately twice the values obtained by using the solution of three-dimensional (spheres) diffusion equation, which would yield incorrect values.

Theoretical Basis for Calculating Micropore-Size Distribution

To date, there are no satisfactory techniques for characterizing the pore-size distribution of microporous materials with the pores smaller than approximately 10 Å. The approach adopted in this study was to combine molecular probing and adsorption isotherm (of N_2 at 77 K) to obtain an estimate of the pore-size distribution.

For a homogeneous or nearly homogeneous microporous material, the Dubinin-Radushkevich (DR) adsorption equation is applicable:

$$W = W_o \exp\left[-B\left(\frac{T}{\beta}\right)^2 \left(\ln\frac{P_s}{P}\right)^2 \right] = f(B) \tag{1}$$

where W is the amount adsorbed at pressure P, β is the affinity coefficient usually based on $\beta = 1$ for benzene as the reference sorbate. B is a structural parameter that increases with an increase in pore size. An empirical relationship was found between B and the half-width x of the slit-like micropores (Dubinin and Stoeckli, 1980; Jaroniec and Madey, 1988) as expressed by:

$$B = kx^2 \tag{2}$$

where the constant K is the characteristic of the sorbent material.

The value of k for Zr-PILC can be determined by using the limiting probe molecule, i.e., the largest molecule that can adsorb in a detectable amount. The limiting probe for Zr-PILC is 1,3,5-trimethyl benzene (TMB), which has a kinetic diameter of approximately 8 Å. Thus, for TMB, the Zr-PILC has a uniform and narrow pore size range of $x = 4$ Å. The value of k, once determined from the TMB data, is a constant for the Zr-PILC and can be used for other gases.

For materials with a distribution of pore sizes, the amount adsorbed is (Stoeckli, 1977):

$$W = \int_o^\infty f(B)G(x)dx \tag{3}$$

where $G(x)$ is the pore-size distribution function. For a Gamma-type distribution function,

$$G(x) = \frac{2(kq)^{n+1}}{\Gamma(n+1)} x^{2n+1} \exp(-kqx^2) \tag{4}$$

the following solution was obtained by Jaroniec et al. (1989), referred to as the Jaroniec-Choma isotherm:

$$\frac{W}{W_o} = \left[\frac{q}{q + \left(\frac{RT}{\beta}\ln\frac{P_s}{P}\right)^2} \right]^{n+1} \tag{5}$$

Based on the above theoretical framework, the procedure for calculating the pore-size distribution is as follows:

1. Determine affinity coefficients β from the D-R equation for the two limiting molecules, TMB and N_2, using benzene as the reference. N_2 is taken as the small molecule that can access all pore sizes in Zr-PILC.
2. Determine the constant k for Zr-PILC by using the D-R equation and the TMB adsorption data.
3. Fit the N_2 adsorption data (at 77 K) to the Jaroniec-Choma isotherm to obtain the values of the constants n and q.
4. From the values of k, n and q, the pore-size distribution is readily calculated from Eq. 4.

Results and Discussion

Sorbent characterization

Table 1 shows the chemical compositions of the montmorillonite clay and three high-surface area Zr-pillared clays obtained by ICP analysis. The conditions for the synthesis of the three Zr-PILC, designated Zr-PILC-2, 4 and 6, were identical (as given above) except for pH during the ion exchange. The pH values for preparing the three samples were 1.4, 4.6, and 8.4, respectively. From the data in Table 1, it is seen that during intercalation, the alkali and alkaline earth cations (mainly Na^+) were exchanged by the tetramers of Zr, $Zr_4(OH)_{14}(H_2O)_{10}^{2+}$ (Baes and Mesmer, 1976; Bartley, 1988).

The cation exchange capacity (CEC) of the montmorillonite clay can be calculated from the chemical composition, because only Na^+, Ca^{+2}, and K^+ (in Table 1) can be exchanged (Moore and Reynolds, 1988). The CEC was 103 meq/100 g. The sample Zr-PILC-2 was nearly 90% exchanged, whereas the other two samples were less exchanged.

The XRD patterns of the montmorillonite and the three Zr-PILC samples are shown in Figure 1. The d_{001} peak for the unpillared clay was at $2\theta = 7.8°$. There is no evidence of this peak in the patterns for the pillared clays, indicating all PILCs were pillared. The peak position of the d_{001} reflection was $2\theta = 3.7°$ for all three Zr-PILCs giving a d_{001} spacing of 23.85

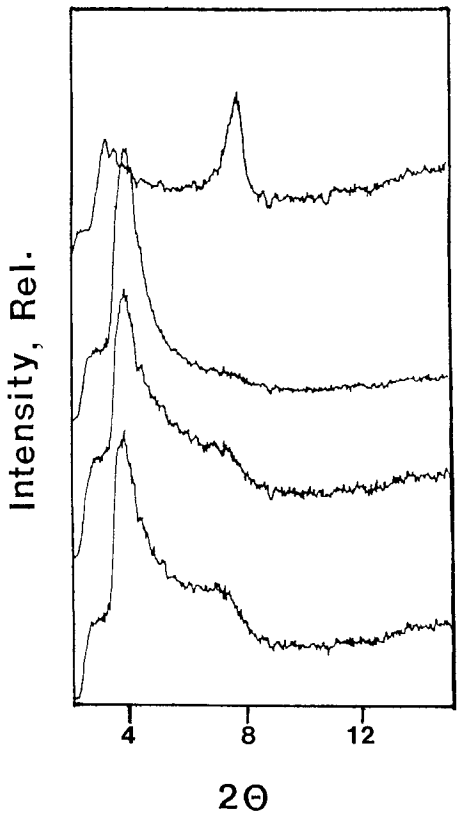

Figure 1. X-ray powder patterns (CuKα source) (from top to bottom): clay, Zr-PILC-2, Zr-PILC-4, and Zr-PILC-6 (all calcined at 350°C).

Å. The free interlayer spacing was obtained by subtracting 9.6 Å, the thickness of the clay layer, from 23.85 Å, giving the value of 14.3 Å. The height of each hydrolyzed Zr tetramer is approximately 10 Å (Bartley, 1988) before dehydration. Thus, the free interlayer spacing of 14.3 Å indicated that the pillars were formed by two back-to-back Zr tetramers, since upon dehydration the tetramer size decreased and 7 Å seems to be a reasonable size for the dehydrated tetramer.

The surface areas and pore volumes of the pillared clays and their ion exchange conditions are summarized in Table 2. The ion exchange conditions differed in the "ligand number," OH/Zr, which was the ratio of the total amounts used in the beginning of ion exchange, and the pH value during the ion exchange process, which was nearly constant. The ratios (in volume) of the solutions 0.1 M $ZrOCl_2$/0.1 M NaOH for the three Zr-PILCs were (for nos. 2, 4 and 6, respectively): 25/5, 25/25, and 25/40. All other conditions were identical, as described above. The surface areas were calculated from the N_2 adsorption (at 77 K) data. One of the surface areas listed in Table 2 was obtained by the α_s method. This method is an empirical method used for the analysis of adsorption in micropores and mesopores and is often used as a check for the validity of the BET surface area (Gregg and Sing, 1982). The unpillared clay was chosen as the reference material in using the α_s method for its chemical similarity to the pillared clays. The N_2 pore volume was measured by N_2 adsorption at 77 K and by taking the limiting pore volume (W_o) in fitting the Dubinin-Astakhov (D-A) equation:

Table 2. Physical Characterization of Zr-PILC: Surface Areas and Pore Volumes vs. Ion Exchange Conditions

Zr-PILC	OH/Zr	pH	BET m^2/g	Langmuir m^2/g	α_s Method m^2/g	N_2 cm^3/g	*n*-Hexane cm^3/g	Benzene cm^3/g
2	0.2	1.4	321.8	499.2	485.7	0.175	0.121	0.108
4	1.0	4.6	195.7	371.9	361.8	0.120	0.069	—
6	1.6	8.4	163.9	359.0	317.9	0.108	0.077	0.057

$$W = W_o \exp\left[-B\left(\frac{T}{\beta}\right)^n \left(\ln \frac{P_s}{P}\right)^n \right] \tag{6}$$

The value of the exponent n is related in a complicated way to the pore-size distribution. The values of n for the three Zr-PILCs (nos. 2, 4 and 6, respectively) were: 3.1, 2.6, and 2.3, indicating structural heterogeneity. The corresponding values of BT/β were 0.408, 0.680, and 0.795.

The BET model is based on multilayer adsorption, which obviously is not applicable to micropores of sizes of a few molecular dimensions. The Langmuir isotherm assumes monolayer adsorption. Therefore, the BET surface area is an underestimate, whereas the Langmuir value is an overestimate. The agreement between the Langmuir surface area and the value from the α_s method indicates that these values are more realistic than the BET values. Table 2 also shows the pore volumes measured by equilibrium pore filling with N_2 (77 K), *n*-hexane (298 K) and benzene (298 K). The higher values obtained with N_2 indicate that there were small pores that were not accessible to *n*-hexane and benzene and that the N_2 values were more realistic. The comparison between the pore volumes is similar to that obtained by Occelli et al. (1985), where the absorbate volumes of the *n*-C_5 to *n*-C_{10} alkanes in an alumina pillared clay were 60–70% of the pore volume.

Tailoring interpillar spacing

The micropore-size distribution was calculated by following the steps described above. By fitting the isotherm data on Zr-PILC to the D-R equation for N_2, benzene and 1, 3, 5-trimethyl benzene, the affinity coefficients, β, for N_2, and TMB were, respectively, 0.31 and 1.43 (β for the benzene standard was 1). The β values for N_2 and 1, 3, 5-triethyl benzene on activated carbon are 0.33 and 1.26, respectively (Dubinin and Stoeckli, 1980), which compare closely with the above values. From the TMB data, the characteristic constant k (in Eq. 2) for Zr-PILC was obtained as 0.0355 $mol^2 \cdot kJ \cdot nm^{-2}$. The values of the constants n and Q for the different Zr-PILCs were then calculated from N_2 adsorption and the pore-size distribution functions, $G(x)$, were obtained from Eq. 4. Figure 2 shows the $G(x)$ functions for the three Zr-PILCs. The $G(x)$ function is nearly Gaussian, slightly skewed toward the righthand side. The area under the curve is unity. The $G(x)$ function is calculated, not actually measured. Other functions have also been assumed, e.g., Gaussian and Rayleigh (Jaroniec and Madey, 1988). However, the solution based on the Gamma-type function is the simplest to use. The $G(x)$ function shown in Figure 2 is a reasonable distribution. Inasmuch as the same basis is used for calculating the $G(x)$ function for all Zr-pillared clays, one

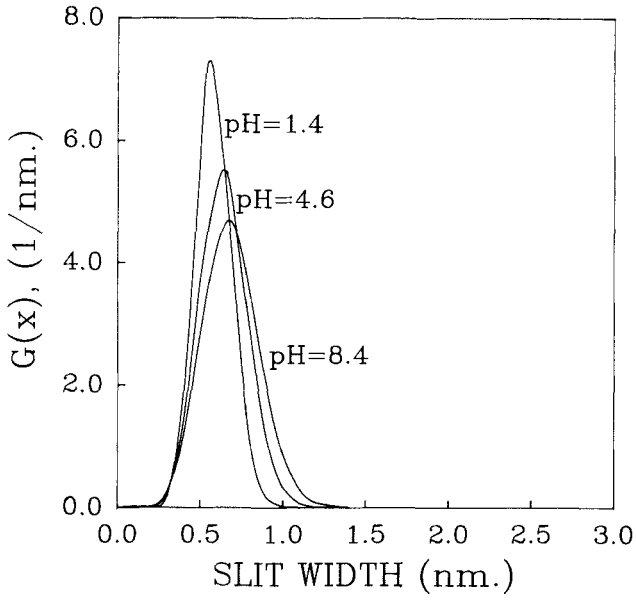

Figure 2. Micropore-size distributions for Zr-PILC nos. 2, 4 and 6 (from left to right) calculated by molecular probing and N_2 (77 K) isotherm.

The slit width is the interpillar spacing.

may proceed to discuss the variables that can be controlled to produce pillared clays with different pore-size distributions.

The peak slit widths in the $G(x)$ distribution were much less than the interlayer spacing, 14.3 Å. Thus, the gallery in the Zr-PILC consisted of narrow and tall paths, limited by the interpillar spacing.

Three conditions in ion exchange were found to influence the interpillar spacing in the resulting Zr-PILC. The first condition was pH. Figure 2 shows that as the pH of the pillaring solution increased, the interpillar spacing also increased. Results in Table 1 indicated that such an increase in interpillar spacing was caused by a decrease in the density of pillars inserted in the interlayer space. This result is consistent with the fact that the concentration of the Zr tetramers increases with decreasing pH in the solution (Baes and Mesmer, 1976). The second obvious variable was the concentration of the Zr solution. Decreasing the concentration from 0.1 M to 0.05 M (keeping the same pH = 1.4) resulted in a significant increase in the interpillar spacing, as shown in Figure 3. This again was attributed to a decrease in the density of pillars. The third variable that one might use to change the interpillar spacing was the addition of a competitive (with Zr tetramers) foreign cation to the solution. Ca^{+2} has a high affinity (higher than Na^+) toward the cation sites in clays (Moore and Reynolds, 1988). By adding Ca^{+2} cations to the 0.05 M $ZrOCl_2$ solution (to 0.1 M Ca^{+2}), the interpillar spacing was further increased as shown in Figure 3.

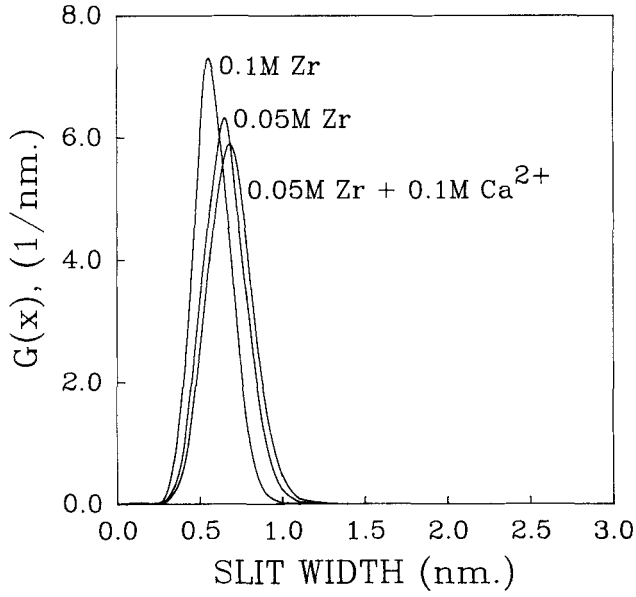

Figure 3. Effects of concentration of ion-exchange solution and addition of a competing cation (Ca^{+2}) on micropore-size distribution.

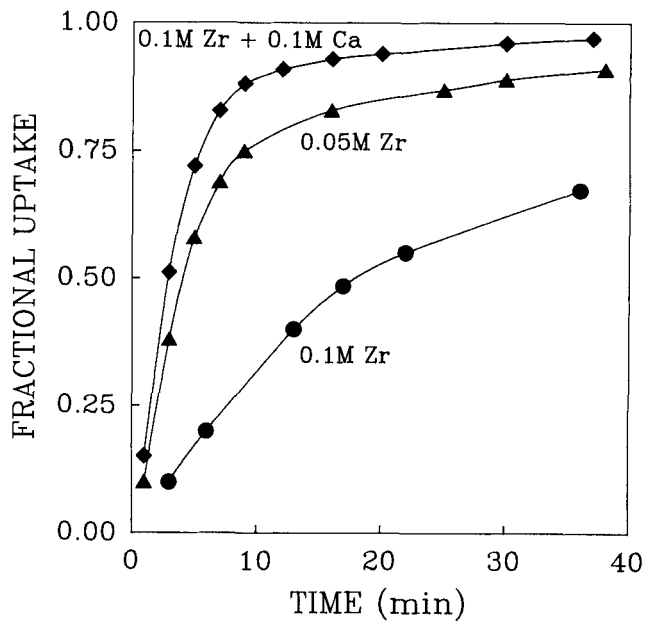

Figure 4. Diffusion (uptake) rates of benzene at 298 K in Zr-PILC prepared by ion exchange at the same pH and OH/Zr, but with different concentrations and Ca^{+2}.

All samples have the same BET surface area.

Figures 2 and 3 show that by changing the three variables, the peak interpillar spacing may be shifted by nearly 2 Å (from nearly 5 Å to nearly 7 Å), a large shift indeed for kinetic separation. Larger shifts may be made in either direction by using a combination of the three variables. The effects of the shift in interpillar spacing on the uptake rate of benzene are illustrated in Figure 4. Comparing the no. 2 Zr-PILC and the sample prepared with 0.05 M $ZrOCl_2$ and 0.1 M Ca^{+2} solution, the diffusion time constant varied by a factor of approximately 15.

Isotherms and diffusivities

The equilibrium isotherms for N_2 and O_2 at 298 K on Zr-PILC-2 are shown in Figure 5. Also included in the figure for comparison are the data for 5A zeolite which is widely used for air separation. The data on 5A were also measured in our

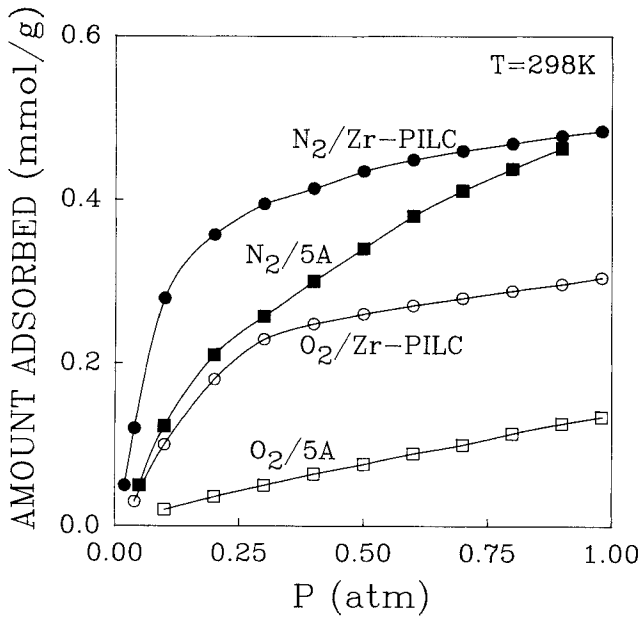

Figure 5. Equilibrium isotherms of N_2 and O_2 on Zr-PILC-2 compared with 5A zeolite.

laboratory. The isotherms for other Zr-PILCs (nos. 4 and 6) for N_2/O_2 as well as other gases/vapors were slightly lower and are not shown here. The equilibrium selectivity for N_2/O_2 on 5A zeolite is approximately 3, high enough for producing high-purity O_2 from air. The N_2/O_2 equilibrium selectivity on Zr-PILC is clearly not high enough for equilibrium air separation. Figure 5 also shows a crossover of the two N_2 isotherms at approximately 1 atm. This is the result of the limiting interpillar spacing in Zr-PILC, not allowing multilayer buildup (which is allowed in the cavities of the 5A zeolite).

The isotherms for water and hydrocarbons in Zr-PILC-2 at 298 K are summarized in Figure 6, which also includes the

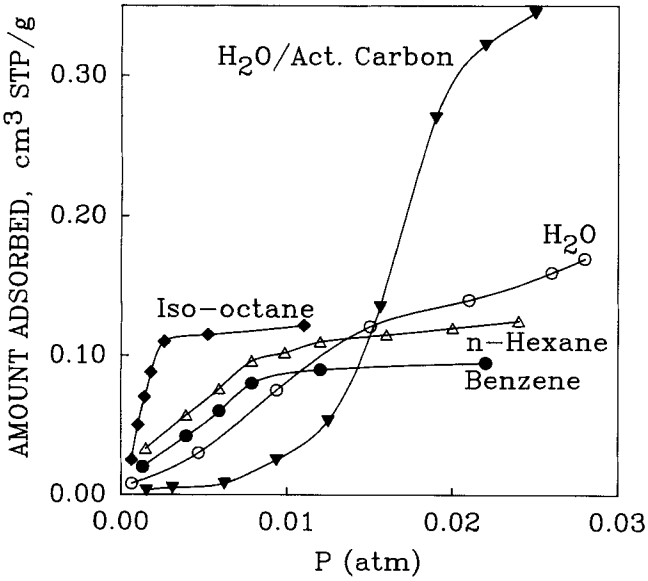

Figure 6. Equilibrium isotherms at 298 K of water and hydrocarbons on Zr-PILC-2 and water on activated carbon.

Table 3. Diffusion Time Constants Calculated from Spherical and Cylindrical Models for Various Adsorbates in Zr-PILC-2 at 298 K

Adsorbate	Critical Size (Å)	D/r^2 (s^{-1}) Sphere	D/r^2 (s^{-1}) Cyl.
Carbon Dioxide	3.3	8.0×10^{-2}	1.53×10^{-1}
Oxygen	3.5	2.74×10^{-2}	5.24×10^{-2}
Nitrogen	3.6	1.50×10^{-3}	2.92×10^{-3}
Methane	3.8	1.10×10^{-3}	2.16×10^{-3}
n-Hexane	4.9	8.94×10^{-4}	1.73×10^{-3}
Benzene	6.7	3.08×10^{-5}	6.20×10^{-5}
p-Xylene	6.7	1.03×10^{-5}	2.02×10^{-5}
Ethylbenzene	6.6	2.11×10^{-6}	4.12×10^{-6}
m-Xylene	7.4	1.41×10^{-6}	2.73×10^{-6}
o-Xylene	7.4	1.21×10^{-6}	2.37×10^{-6}
1,3,5-TMB	8.6	9.38×10^{-7}	1.84×10^{-6}

water isotherm in activated carbon for comparison. Compared with the water isotherms on A-type and the X-type zeolites, silica gel and activated alumina (Yang, 1987), Zr-PILC is substantially less hydrophilic. And it is slightly more hydrophilic than silicalite. Thus, Zr-PILC may be characterized as a mildly hydrophobic sorbent and could be used for aqueous applications. Figure 6 also shows the isotherms for two paraffins and an aromatic, all exhibiting micropore-filling behavior.

The diffusivities of different gases are expressed as the re-

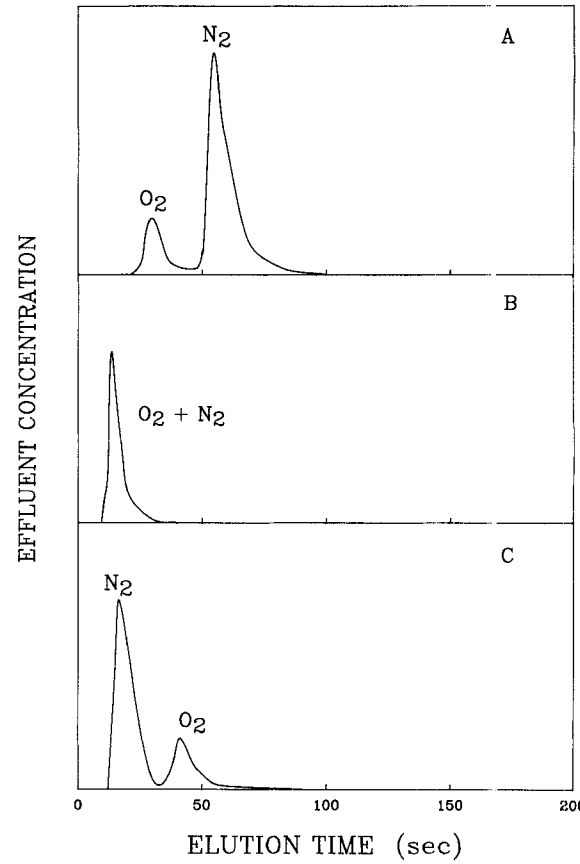

Figure 7. Chromatographic air separation in a column of Zr-PILC-2 at 298 K at space velocities of: (A) 1.05 min^{-1}, (B) 3.14 min^{-1}, (C) 4.16 min^{-1}.

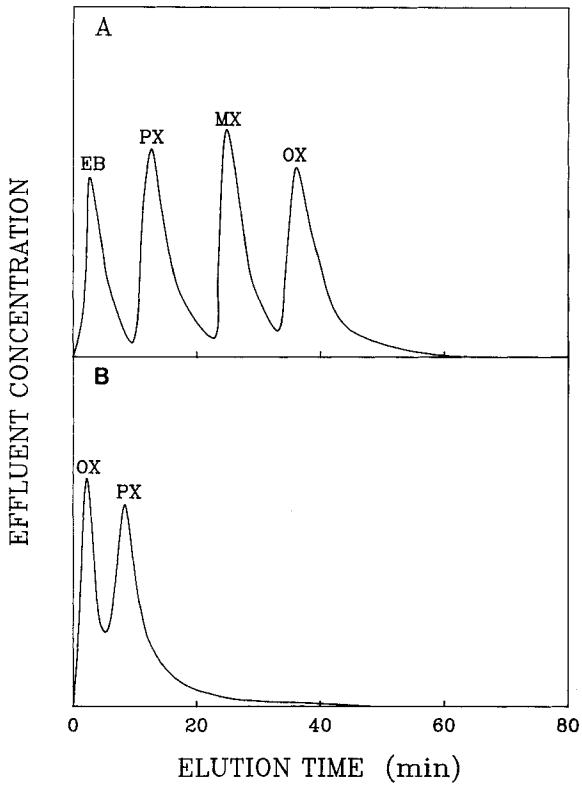

Figure 8. Chromatographic separation of ethyl benzene (EB), paraxylene (PX), metaxylene (MX) and orthoxylene (OX) by Zr-PILC-2 at 503 K at space velocities of: (A) 12.03 min^{-1} and (B) 105.9 min^{-1}.

ciprocals of time constants, D/r^2, shown in Table 3. These values were calculated from the uptake rates using the solution for the two-dimensional diffusion equation. The mean crystal disc radius was less than 2 μm. Of particular interest to this work was the feasibility for air separation using Zr-PILC. The results showed that the ratio of the diffusivities of $O_2/N_2 = 17.9$, which is clearly adequate for kinetic separation.

Chromatographic separation

The feasibility for air separation was examined by chromatographic separation. The elution curves from columns packed with Zr-PILC-2 particles are shown in Figure 7, as signal from a thermoconductivity detector vs. retention time. The particles were 80–100 mesh agglomerated crystals. In each run, a 1-cm^3 air sample was injected into the helium carrier. All runs were carried out at a column temperature of 25°C. Figure 7A is the result obtained under the following conditions: 1/8-in. (3.17-mm)-ID column, 4-ft (122-cm)-long, 5.2-g Zr-PILC-2; carrier flow rate = 10 cm^3(NTP)/min. The same column and same conditions were used for the results shown in Figure 7B, except that the carrier flow rate was increased to 30 cm^3(NTP)/min. The column used for 7C was 1/4-in. (6.34-mm)-ID, 18-in. (45.7-cm)-long, containing 9.5-g Zr-PILC-2, with a carrier flow rate of 60 cm^3(NTP)/min. The larger-diameter column was used for the higher flow rate to avoid an excessively large pressure drop. Upstream pressures were 2, 2 and 3 atm, respectively, for the runs shown in 7A, 7B and 7C. The 7A result was caused by equilibrium difference. As the space velocity increased, the diffusion resistance (into the interpillar spacing) became important and the separation shifted from equilibrium to kinetic, where a total reversal of the elution curves occurred. It should be noted that the linear flow velocity cannot be taken as a criterion for judging the relative importance of diffusion resistance vs. equilibrium affinity for determining the order of elution.

Figure 8 shows the chromatograms of xylene isomers. Figure 8A is the result of separation of ethyl benzene and xylene isomers: ethyl benzene (EB), paraxylene (PX), metaxylene (MX) and orthoxylene (OX). A 1/4-in. (6.34-mm) column (8.89-cm-long) containing 2.4-g Zr-PILC-2 was used. One μL containing equal concentrations of the four compounds was injected in a helium flow of 20 cm^3/min. The four compounds were separated based on their equilibrium adsorption affinity: OX > MX > PX > EB. Figure 8B shows the result of kinetic separation of OX and PX. Although OX is more strongly adsorbed than PX, the diffusivity of PX is significantly higher than OX (see Table 3). The chromatographic separation is based on the diffusivity difference. In this experiment, a 1/8-in. (3.17-mm) column (6-in. or 15.24-cm) containing 0.65-g Zr-PILC-2 was used. A 0.5-μL sample with equal concentrations of OX and PX was injected into a He flow of 75 cm^3/min. Kinetic separations of other mixtures of these four compounds have also been tried without success, due to the close proximity of their diffusivities.

Acknowledgment

This work was supported by NSF under grant no. CTS-8914754.

Notation

B = structural parameter
D = diffusivity
k = constant in Eq. 2
n = constant in Eq. 4
P = pressure
P_s = saturated vapor pressure
q = constant in Eq. 4
r = radius of crystal discs
R = gas constant
T = absolute temperature
W = amount adsorbed
W_o = saturated amount adsorbed
x = half-width of slit-shaped pores, interpillar spacing

Greek letter

β = affinity coefficient

Literature Cited

Ackley, M. W., and R. T. Yang, "Kinetic Separation by Pressure Swing Adsorption: Method of Characteristic Model," *AIChE J.*, **36**, 1229 (1990).

Baes, C. F., and R. E. Mesmer, *The Hydrolysis of Cations*, Wiley, New York (1976).

Bandosz, T., J. Jagiello, and M. Zyla, "Studies of the Chemical Character of Surface of Smectite Intercalated with Hydroxy-alumina," *Chemia Stosowana*, **33**, 189 (1989).

Bartley, G. J. J., "Zirconium Pillared Clays," *Catalysis Today*, R. Burch, ed., Elsevier, New York (1988).

Brindley, G. M., and R. E. Semples, "Preparation and Properties of Some Hydroxy-Aluminum Beidellites," *Clay Minerals*, **12**, 229 (1977).

Burch, R., ed., "Pillared Clays," *Catalysis Today*, **2**, 185, Elsevier, New York (1988).
Clearfield, A., "Recent Advances in Pillared Clays and Group IV Metal Phosphates," *NATO ASI Ser.*, Ser. C, **231**, 271 (1988).
Drezdon, M. A., "Synthesis of Isopolymetalate-Pillared Hydrotalcite via Organic-Anion-Pillared Precursors," *Inorg. Chem.*, **27**, 4628 (1988).
Dubinin, M. M., and H. F. Stoeckli, "Homogeneous and Heterogeneous Micropore Structures in Carbonaceous Sorbents," *J. Coll. Interf. Sci.*, **75**, 34 (1980).
Figueras, F., "Pillared Clays as Catalysts," *Catal. Rev. Sci. Eng.*, **30**, 457 (1988).
Gregg, S. J., and K. S. W. Sing, *Adsorption, Surface Area and Porosity*, 2nd ed., Academic Press, New York (1982).
Jaroniec, M., and R. Madey, *Physical Adsorption on Heterogeneous Solids*, Elsevier, New York (1988).
Jaroniec, M., R. Madey, J. Choma, B. McEnaney, and T. J. Mays, "Comparison of Adsorption Methods for Characterizing the Microporosity of Activated Carbons," *Carbon*, **27**, 77 (1989).
Jones, S. L., "The Preparation and Solution Chemistry of Al and Zr Pillaring Species," *Catalysis Today*, R. Burch, ed., Elsevier, New York (1988).
Kapoor, A., and R. T. Yang, "Kinetic Separation of CH_4–CO_2 by Adsorption on Molecular Sieve Carbon," *Chem. Eng. Sci.*, **44**, 1723 (1989).
Lahav, N., N. Shani, and J. Shabtai, "Cross-Linked Smectite. 1. Synthesis and Properties of Hydroxy-Aluminum-Montmorillonite," *Clays Clay Miner.*, **26**, 107 (1978).
Loeppert, R. H., M. M. Mortland, and T. J. Pinnavaia, "Synthesis and Properties of Heat-Stable Expanded Smectite and Vermiculite," *Clays Clay Miner.*, **27**, 201 (1979).
Moore, D. M., and R. C. Reynolds, Jr., *X-Ray Diffraction and the Identification and Analysis of Clay Minerals*, Oxford University Press, Oxford (1989).
Occelli, M. L., R. A. Innes, F. S. S. Hwu, and J. W. Hightower, "Sorption and Catalysis on Sodium-Montmorillonite Interlayered with Aluminum Oxide Clusters," *Appl. Catal.*, **14**, 69 (1985).
Occelli, M. L., and R. M. Tindwa, "Physical Chemical Properties of Montmorillonite Interlayered with Cationic Oxyaluminum Pillars," *Clays Clay Miner.*, **31**, 22 (1983).
Pan, Z., R. T. Yang, and J. A. Ritter, "Kinetic Separation of Air by PSA," *New Directions in Sorption Technology*, G. E. Keller, Jr., and R. T. Yang, eds., Butterworth, Boston (1989).
Pinnavaia, T. J., "Intercalated Clay Catalysts," *Sci.*, **220**, 365 (1983).
Pinnavaia, T. J., M. S. Tzou, S. D. Landau, and R. H. Raythatha, "On the Pillaring and Delamination of Smectite Clay Catalysts by Polyoxo Cations of Aluminum," *J. Mol. Catal.*, **27**, 195 (1984).
Sahimi, M., T. T. Tsotsis, and M. L. Occelli, "Computer Simulation of Diffusion, Adsorption and Reaction of Organic Molecules in Pillared Clays," *Mater. Res. Soc. Symp. Proc.*, **111**, 271 (1988).
Shabtai, J., R. Lazar, and A. G. Oblad, *Proc. Int. Cong. Catalysis*, T. Seiyama and K. Tanabe, eds., 828, Elsevier, Tokyo/Amsterdam (1980).
Shabtai, J., M. Rosell, and M. Takarz, "Cross-Linked Smectites: III. Synthesis and Properties of Hydroxy-Aluminum Hectorites and Fluorhectorites," *Clays Clay Miner.*, **32**, 99 (1984).
Shin, H.-S., and K. S. Knaebel, "Pressure Swing Adsorption: An Experimental Study of Diffusion-Induced Separation," *AIChE J.*, **34**, 1409 (1988).
Sprung, R., M. E. Davis, J. S. Kauffman, and C. Dybowski, "Pillaring of Magadiite with Silicate Species," *Ind. Eng. Chem. Res.*, **29**, 213 (1990).
Sterte, J., "Hydrothermal Treatment of Hydroxycation Precursor Solutions," *Catalysis Today*, R. Burch, ed., Elsevier, New York (1988).
Stoeckli, H. F., "A Generalization of the D-R Equation for the Filling of Heterogeneous Micropore Systems," *J. Coll. Interf. Sci.*, **59**, 184 (1977).
Tzou, M. S., and T. J. Pinnavaia, "Chromia Pillared Clays," *Catalysis Today*, R. Burch, ed., 243, Elsevier, New York (1988).
Vaughan, D. E. W., R. J. Lussier, and J. S. Magee, "Pillared Interlayered Clay Materials Useful as Catalysts and Sorbents," U.S. Patent 4,176,090 (1979).
Yamanaka, S., and M. Haltori, "Iron Oxide Pillared Clays," *Catalysis Today*, R. Burch, ed., 261, Elsevier, New York (1988).
Yang, R. T., *Gas Separation by Adsorption Processes*, Butterworth, Boston (1987).
Yeh, Y. T., and R. T. Yang, "Diffusion in Zeolite Containing Mixed Cations," *AIChE J.*, **35**, 1659 (1989).

Manuscript received Oct. 16, 1990, and revision received Mar. 11, 1991.